Constrained, aqueous growth of three-dimensional single crystalline zinc oxide structures

Kathryn J. Pooley,[a] John H. Joo, and Evelyn L. Hu
School of Engineering and Applied Sciences, Harvard University, Cambridge, Massachusetts 02138, USA

(Received 10 December 2013; accepted 9 January 2014; published online 28 January 2014)

We study low temperature (90 °C) aqueous growth of single crystal zinc oxide structures through patterned PMMA molds of different sizes, shapes, and orientations. We demonstrate the ability to create 3D shapes with smooth vertical sidewalls. Although the unconstrained growth is influenced by the hexagonal geometry of the underlying crystal structure, the ZnO is shown to conform exactly to any shape patterned. Using electron backscatter diffraction and scanning electron microscopy we show that the mold orientation, in conjunction with control of the growth rates of the c and m planes of the ZnO, is crucial in determining the final structure shape. [http://dx.doi.org/10.1063/1.4863075]

Selective growth of semiconductor materials through pre-patterned masking layers can provide important advantages for the definition and performance of the final structures. Such an approach can control the placement of arrays of microstructures or nano-structures.[1–5] Selective growth of optical waveguides or resonators could result in structures with crystallographically smooth sidewalls, and without the challenges of degradation brought about by an etch process.[6–9] In many cases, patterned, epitaxial growth of high quality semiconductor materials occurs only at high temperatures (typically $> 500\,^{\circ}$C), making the masking and control of the growth process difficult.[10,11] This work explores the selective growth of single crystal zinc oxide (ZnO), formed through a low temperature, aqueous process where the growth is directed by nanometer-scale and micron-scale pre-patterned "molds" formed of electron-beam resist. The effects of the mask material on the constrained growth, size and shape of the pre-patterned opening, as well as the orientation of the mask with respect to the underlying crystalline structure are investigated. The structures we fabricate demonstrate the ability to easily control the final 3D shape of the grown ZnO simply by controlling the growth duration and strategically choosing the size, shape, and orientation of the masking material.

ZnO is a transparent, wide bandgap (~3.3 eV) semiconductor, with a predominant hexagonal wurtzite crystalline structure at ambient conditions.[12] A variety of techniques have been employed to form ZnO.[13] Our approach incorporates a solution-based growth in zinc nitrate hexahydrate, ammonium hydroxide, sodium citrate, and deionized water similar to previous reports.[14–17] The process is described in detail in Ref. 14. A seed layer was first formed on lattice matched (111) $MgAl_2O_4$ spinel substrates under microwave treatment. Samples were then placed in a 90 °C oven overnight to form the base layer. The base layer was lithographically patterned with e-beam resist, resulting in polymer-based "molds" of different shapes and orientations. Further growth of ZnO was carried out at 90 °C in a conventional oven.

Initial experiments utilized four different diameter circular molds (2 μm, 1 μm, 500 nm, and 200 nm) formed of ~500 nm thick patterned polymethylmethacrylate (PMMA). ZnO was grown for 4 h, with an 8 M zinc nitrate growth solution. The final structure which was grown through the 200 nm pattern is shown in Figure 1(a). For all of the grown structures the ZnO fully fills the circular

[a]Author to whom correspondence should be addressed. Electronic mail: greenber@fas.harvard.edu

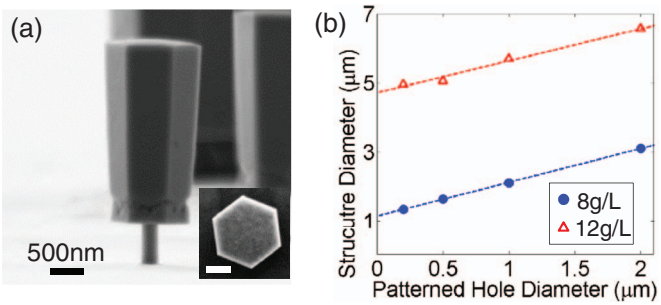

FIG. 1. (a) SEM micrograph of ZnO grown in an 8 M zinc nitrate growth solution for 4 h through a 200 nm diameter circular hole. Inset shows top-down view of ZnO structure with the scale bar equal to 500 nm. (b) Comparison of the size of ZnO structures grown through patterned circular openings with both 8 M (blue circles) and 12 M (red triangles) zinc nitrate growth solutions.

molds and assumes the shape of the post region. The final height of the hexagonal structures grown through all four patterned diameter sizes was found to be the same (3.6 ± 0.1 μm), unaltered by the size of the hole opening. Therefore, the growth rate in the (0001) direction dominates the ZnO growth. Once the growth reaches the top of the mold and is laterally unconstrained, the "natural" hexagonal symmetry of the ZnO structures emerges and the sidewalls of the overgrown region become smooth with crystallographically-defined m-plane facets. Figure 1(b) shows that a linear dependence between the hole opening and the final structure diameter is observed. Regardless of the diameter of the post, the lateral overgrowth of the structure is 0.55 ± 0.04 μm. This indicates a lateral growth rate independent of the mold size and shape, which is determined by the rate of growth perpendicular to each (slow-growing) m-plane facet. Therefore, we conclude that the ZnO growth is determined by the c-plane growth in the vertical direction and by the m-plane growth in the lateral direction.

The exact growth rate of the various ZnO crystalline planes is non-trivial to calculate due to the fact that the rate is nonlinear. The patterned samples require some time to come to thermal equilibrium with the 90 °C oven temperature. Growth will occur when the increased temperature results in the decreased solubility of ZnO in solution.[18] Preliminary experiments established that the ZnO growth begins 2 h after the sample is placed in the oven. If we assume a subsequent constant growth rate, the vertical (0001) c-axis growth rate of the ZnO is calculated to be ~30 nm/min. In addition using the same assumptions and taking into account the time required to grow to the top of the patterned mold, the growth rate of the $(10\bar{1}0)$ m-planes is found to be ~6 nm/min. These two rates may be separately controlled by changing the concentration of the zinc nitrate and/or the sodium citrate in the growth solution. For the same growth time, changing the concentration of zinc nitrate in the growth solution to 12 M resulted in an increased height of the structures to 6.8 ± 0.30 μm and an additional lateral epitaxial overgrowth to 2.32 ± 0.05 μm for all four hole openings. This corresponds to growth rates in the vertical and lateral directions of ~57 nm/min and ~21 nm/min, respectively. The linear relationship between the patterned hole diameter and final structure diameter for the higher concentration solution is shown in Figure 1(b).

We then altered the shapes of the molds and investigated the geometry of the resulting ZnO structures. Several different shapes (circle, hexagon, triangle, and square) each with a lateral dimension d of 3 μm as shown in Figure 2 were patterned in the approximately 500 nm thick PMMA to create molds for the ZnO growth. The upper and lower SEM images in Figure 2 show the resulting structures after 4 h of growth, imaged perpendicular to the plane of the substrate and at a 6.5° angle from the substrate, respectively. The bottom part of the ZnO structure, which is visible in the lower SEM images in Figure 2 and which we will refer to as the post, again exactly fills the mold that was patterned. Similar to the results obtained for the circular molds, once the thickness of the ZnO exceeds the height of the mask layer the growth is no longer constrained in the lateral direction, and the natural hexagonal symmetry of the ZnO structures emerges, as is evident in Figure 2.

The clear hexagonal symmetry of the ZnO structure suggests that there is a defined crystallographic orientation in the material that guides the growth of the structures, perhaps present in

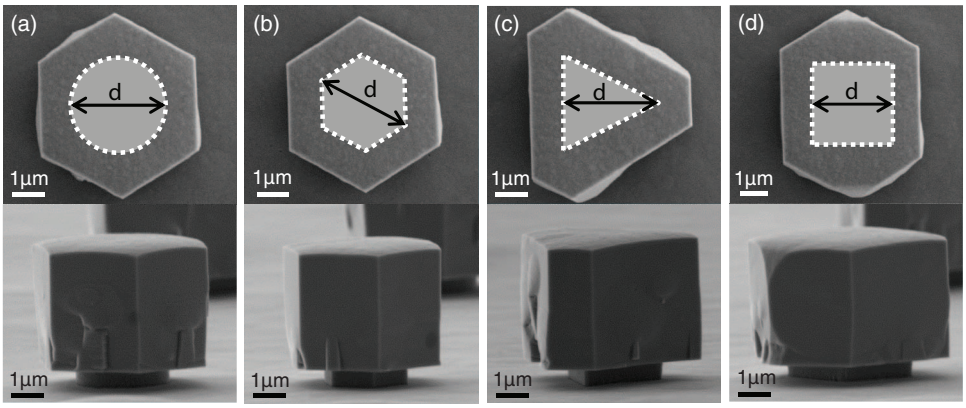

FIG. 2. Scanning electron microscopy images taken perpendicularly to the substrate (upper images) and at a tilt of 6.5° from the substrate (lower images) of the resulting ZnO structures after 4 h of growth in a 90 °C oven with initially patterned (a) circle, (b) hexagon, (c) triangle, and (d) square. Outlined shaded region indicates the e-beam lithography patterned post and d = 3 μm.

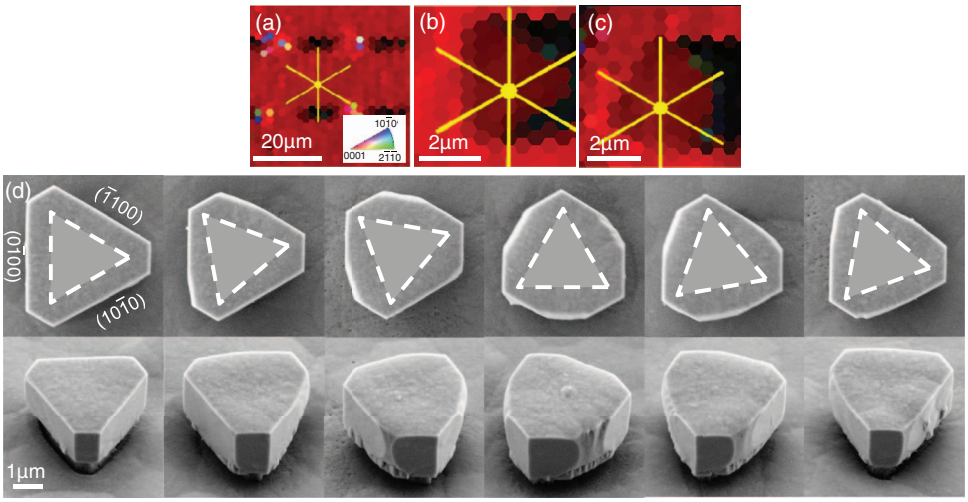

FIG. 3. Successive rotation of e-beam lithography patterned triangular mold with ZnO growth of 3.5 h. (a) Combined image quality (IQ) and inverse pole figure (IPF) obtained using electron backscatter diffraction (EBSD) of the ZnO base layer with the direction of the m-planes of the ZnO indicated with yellow lines. Electron backscatter diffraction combined IQ and IPF of a ZnO structure grown through (b) a mold aligned with the base layer crystalline planes and (c) a mold misaligned from the base layer crystalline planes by 30°. Yellow lines indicate the m-planes of the ZnO. (d) SEM micrographs taken perpendicular to the sample (upper images) and at a 45° tilt angle (lower images) with each pattern from left to right rotated an additional 10°. The first image shows when the mold and therefore the final ZnO structure was aligned with the hexagonal crystalline planes of the ZnO base layer.

the base layer. Such an orientation was confirmed by electron backscatter diffraction (EBSD) measurements, seen in the combined image quality (IQ) and inverse pole figure (IPF) in Figure 3(a). The colors in the figure indicate the collective quality[19] of the electron backscatter diffraction pattern together with the crystal orientations of the material. The m-planes in ZnO are indicated by yellow lines. Given the crystallographic orientation of the base layer, we sought to understand the effect of the orientation of the mold geometry relative to the base layer. These data are shown in Figure 3(d): 3 μm triangular openings were patterned in the PMMA with each successive pattern rotated by 10°. The scanning electron microscope (SEM) images of the resulting structures after 3.5 h of growth show the shape of the overgrown material relative to the orientation of the original mold pattern. Deviations of the mold orientation from that of the ZnO base layer's crystalline structure result in growth of less regular geometrical shapes in the xy-plane. These structures can be

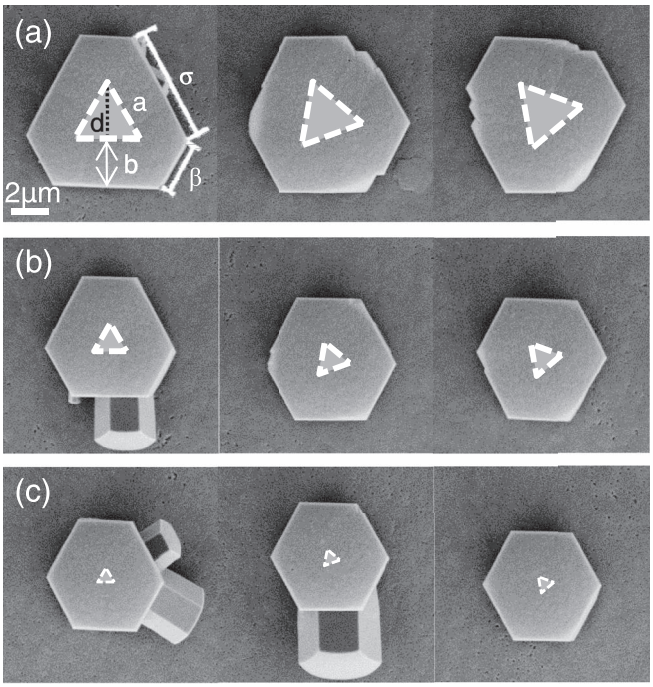

FIG. 4. SEM micrographs of ZnO grown for 4 h through (a) d = 3 μm, (b) d = 1.5 μm, and (c) d = 750 nm patterned triangle in resist. (a is the side length of the triangle, b is the amount of growth perpendicular to the m-plane direction of ZnO, $\sigma = 2\sqrt{3}b(\mathrm{t})/3 + \mathrm{a}$, and $\beta = 2\sqrt{3}b(\mathrm{t})/3$). In each successive SEM image from left to right the patterned triangle was rotated an additional 20° relative to the crystalline planes of the ZnO base layer. Scale is the same for all images.

seen as intermediary shapes, before the overall structures become hexagonal. When the edges of the patterned opening align with the $(10\bar{1}0)$ m-planes of the ZnO, very smooth and vertical sidewalls are observed. The ability to easily form extremely smooth sidewalls is particularly important for optical devices, to minimize scattering loss. These experiments suggest that smooth sidewalls can be obtained, even for non-hexagonal structures and molds, through the judicious orientation of the mold pattern to the base layer.

EBSD measurements performed on the top surface of the grown ZnO structures confirm a common orientation of all the ZnO material relative to the base layer's crystallographic orientation. Figures 3(b) and 3(c) show the combined image qualities and inverse pole figures, as well as measured ZnO m-plane orientations for a mold aligned with the base layer's crystallographic planes and for a mold misaligned by 30° from the crystal structure of the base layer, respectively. Although the initial shape in the xy-plane is heavily influenced by the mold orientation, the m-plane orientation of the ZnO in both figures is the same. This indicates that while the crystalline orientation of the material is always the same, the final shape of the ZnO in the xy-plane can be changed by rotating the mold through which it is grown.

The data shown in Figures 2 and 3 show the dominance of the growth rate perpendicular to the m-planes in producing the hexagonal symmetry in the xy-plane. We wanted to better understand the transition from the lateral shape defined by the mold to the eventual hexagonal shape dictated by the underlying orientation of the base layer. Thus, we combined different size patterned openings and various rotations of the triangular patterns as shown in Figure 4. All of the growth conditions for the structures are kept the same, with a triangular core dimension of d = 3 μm, 1.5 μm, and 0.75 μm, respectively, and growth time of 4 h. Using a simple geometric calculation the length of each edge of the final structure at a given growth time can be calculated. The three edges of the hexagonal structure parallel to those of the patterned triangle have a length of $\sigma = 2\sqrt{3}b(\mathrm{t})/3 + \mathrm{a}$, where $a = 2d\sqrt{3}/3$ is the side length of the patterned triangle and $b(t)$ is the amount of growth perpendicular to the $(10\bar{1}0)$ m-plane direction as a function of time, as shown in the left most

panel of Figure 4(a). The amount of lateral growth, $b(t)$, is found to be independent of the size of the patterned triangle. The remaining three sides of the final ZnO structure, which form from the vertices of the patterned triangle, have a length of $\beta = 2\sqrt{3}b(t)/3$. As expected, these are the same length for the three different size triangles patterned (2.99 ± 0.03 μm). As the size of the patterned triangular openings is reduced, the value of a becomes small compared to $2\sqrt{3}b(t)/3$ and thus the shape in the xy-plane approaches a regular hexagon at earlier times in the growth. Therefore, by choosing a mold for the post region and strategically orienting the mold with respect to the crystalline orientation of the base layer, a variety of three-dimensional ZnO shapes can be grown with high quality sidewalls determined by the crystal facets. In addition, if the diameter of the post is significantly less than the amount of lateral overgrowth then the resulting structures are hexagonal with smooth sidewalls, and have no dependence on the initial mold orientation.

In some of the images in Figure 4 additional ZnO growth on the sides of the structures has occurred and is believed to have resulted from nucleation at specific sites on the lower part of the sidewalls of some of the structures.[20] While the origin of the extra nucleation is currently unknown, the density of the extra nucleation varies between samples which suggests some sort of contamination either in the growth solution or on the surface of the mold utilized. Further investigation is required to control the formation of such extra nucleation, and to further understand how the structure is modified as growth proceeds from constrained (by the mold) to unconstrained.

In conclusion, this work shows the ability to exert control over single crystalline zinc oxide structures aqueously grown through patterned molds of various shapes and sizes. The ZnO precisely fills the molded region during growth regardless of the shape of the mold patterned. As expected, the faster growth rate of the c-plane of the ZnO with respect to the m-plane growth rate has been observed. The m-plane growth determines the lateral shape of the final ZnO structures, and the orientation of the mold with respect to the crystalline planes in the base layer is found to play an important role in the crystal facets observed in the final ZnO structures. By aligning the mold to the crystalline planes in the base layer, smooth, high quality sidewalls are observed. When misaligned, a variety of three-dimensional structures can be fabricated. In addition, when the diameter of the post is much smaller than the lateral overgrowth the final ZnO structures are hexagonal regardless of the orientation of the mold. The ability to easily fabricate ZnO structures with such smooth sides using this patterned aqueous growth technique, and without the use of possibly damaging etching techniques, opens the door to new and improved devices such as microdisks, photonic crystals, and lasers. Good quality material and smooth sidewalls are necessary for many devices as loss and scattering mechanisms need to be kept to a minimum for efficiently operating devices.

This work was facilitated by the Center for Nanoscale Systems (CNS) at Harvard University and the National Science Foundation Graduate Research Fellowship Program. The authors thank Tsung-li Liu for useful discussions and fabrication advice.

[1] J. J. Richardson, D. Estrada, S. P. DenBaars, C. J. Hawker, and L. M. Campos, J. Mater. Chem. **21**, 14417 (2011).
[2] R. R. Li, P. D. Dapkus, M. E. Thompson, W. G. Jeong, C. Harrison, P. M. Chaikin, R. A. Register, and D. H. Adamson, Appl. Phys. Lett. **76**, 1689 (2000).
[3] Y.-J. Kim, C.-H. Lee, Y. J. Hong, G.-C. Yi, S. S. Kim, and H. Cheong, Appl. Phys. Lett. **89**, 163128 (2006).
[4] I. Aharonovich, J. C. Lee, A. P. Magyar, D. O. Bracher, and E. L. Hu, Laser Photon. Rev. **7**, L61 (2013).
[5] D. Andeen, J. H. Kim, F. F. Lange, G. K. L. Goh, and S. Tripathy, Adv. Funct. Mater. **16**, 799 (2006).
[6] S. Murad, M. Rahman, N. Johnson, S. Thoms, S. P. Beaumont, and C. D. W. Wilkinson, J. Vac. Sci. Technol. B Microelectron. Nanom. Struct. **14**, 3658 (1996).
[7] J. S. Park, H. J. Park, Y. B. Hahn, G.-C. Yi, and A. Yoshikawa, J. Vac. Sci. Technol. B Microelectron. Nanom. Struct. **21**, 800 (2003).
[8] E. D. Haberer, R. Sharma, C. Meier, A. R. Stonas, S. Nakamura, S. P. DenBaars, and E. L. Hu, Appl. Phys. Lett. **85**, 5179 (2004).
[9] J. C. Lee, A. P. Magyar, D. O. Bracher, I. Aharonovich, and E. L. Hu, Diam. Relat. Mater. **33**, 45 (2013).
[10] H. P. Sun, X. Q. Pan, X. L. Du, Z. X. Mei, Z. Q. Zeng, and Q. K. Xue, Appl. Phys. Lett. **85**, 4385 (2004).
[11] A. Krost, J. Christen, N. Oleynik, A. Dadgar, S. Deiter, J. Bläsing, A. Krtschil, D. Forster, F. Bertram, and A. Diez, Appl. Phys. Lett. **85**, 1496 (2004).
[12] U. Özgür, Y. I. Alivov, C. Liu, A. Teke, M. A. Reshchikov, S. Doğan, V. Avrutin, S.-J. Cho, and H. Morkoç, J. Appl. Phys. **98**, 041301 (2005).
[13] L. Schmidt-Mende and J. L. Macmanus-Driscoll, Mater. Today **10**, 40 (2007).
[14] J. H. Joo, K. J. Greenberg, M. Baram, D. R. Clarke, and E. L. Hu, Cryst. Growth Des. **13**, 986 (2013).
[15] J. J. Richardson and F. F. Lange, J. Mater. Chem. **21**, 1859 (2011).

[16] D. Andeen, L. Loeffler, N. Padture, and F. F. Lange, J. Cryst. Growth **259**, 103 (2003).
[17] D. B. Thompson, J. J. Richardson, S. P. DenBaars, and F. F. Lange, Appl. Phys. Express **2**, 042101 (2009).
[18] J. J. Richardson and F. F. Lange, Cryst. Growth Des. **9**, 2570 (2009).
[19] S. I. Wright and M. M. Nowell, Microsc. Microanal. **12**, 72 (2006).
[20] T. L. Sounart, J. Liu, J. A. Voigt, M. Huo, E. D. Spoerke, and B. Mckenzie, J. Am. Chem. Soc. **129**, 15786 (2007).